Performance Analysis of an Active Magnetic Regenerative Refrigerator for 20 K

I. Park, S. Jeong

KAIST, Daejeon, Republic of Korea

ABSTRACT

An active magnetic regenerative refrigerator (AMRR) with the conduction cooled high temperature superconducting (HTS) magnet is fabricated and experimentally investigated. Key components of the AMRR are a two-stage multi-layered active magnetic regenerator (AMR), a conduction cooled HTS magnet, and the helium gas flow system. Since magnetic refrigerants are only effective in the limited temperature range near their Curie temperatures, the layered structure with four magnetic materials ($GdNi_2$, $Gd_{0.1}Dy_{0.9}Ni_2$, $Dy_{0.85}Er_{0.15}Al_2$, $Dy_{0.5}Er_{0.5}Al_2$) is employed on the AMR to increase its temperature span. The AMR is designed to operate with the temperature range between 80 K and 20 K. The HTS magnet, being cooled down by a two-stage Gifford-McMahon (GM) cryocooler, produces maximum magnetic field of 3 T for the AMR. DC power supply, a solenoid current switch and an external dump resistor are used for a continuous ramping operation of the HTS magnet. Oscillating helium flow in the AMR is induced and controlled by the helium compressor and four solenoid valves. This paper presents the experimental results of the AMR system operating between 80.8 and 21.8 K and discusses technical issues for the results.

INTRODUCTION

An AMRR is a type of magnetic refrigerator which utilizes magneto-caloric effect (MCE) for refrigeration. Early magnetic refrigerator such as an adiabatic demagnetization refrigerator (ADR) has been only employed to obtain sub-Kelvin temperature [1]. However, adoption of an active magnetic regenerator concept has enabled researchers to use MCE for refrigeration with a large temperature span. An AMR system can achieve much larger temperature lift than that of ADR by effectively utilizing a magnetic refrigerant as a regenerator and as an active magnetic component. Due to its advantage, an enormous number of AMRRs operating at room temperature have been reported [2-4]. However, only a few AMRRs working below liquid nitrogen temperature have been developed and investigated over the past several decades [5 - 11].

Since the energy interaction of MCE is an inherently reversible process, AMRR has high thermodynamic potential to improve the efficiency of hydrogen liquefaction. In order to achieve the wide temperature span of an AMR, large magnetic entropy change over broad temperature range is indispensable [12]. Although an AMR can operate at a larger temperature span than the adiabatic temperature rise of a magnetic refrigerant, the temperature span is still limited because the sufficiently large MCE of a typical magnetic refrigerant appears over a limited temperature range. For instance,

Cryocoolers 19, edited by S.D. Miller and R.G. Ross, Jr.

Numazawa et al. [8] experimentally investigated single layered AMRs with three different kinds of magnetic refrigerants (GGIG, $HoAl_2$, and $DyAl_2$) and the maximum temperature span of 12 K was achieved at the maximum magnetic field of 1.8 T. Moreover, they proposed a three stage AMR to cover the temperature span between 77 K and 20 K. Limitation of a single AMR can be overcome by using a multi-layered AMR. A two stage, two-layered AMR [10, 11] is reported in the previous research with an operating temperature span of 50 K.

An AMR requires magnetic field variation during operation. A superconducting magnet is an appropriate candidate as a magnetic field generator for a cryogenic device such as a hydrogen liquefier. Previous research groups [8, 9] used direct current (DC) superconducting magnet to apply the necessary magnetic field to the AMR. The magnetic field variation of the AMR was possible by relative displacement between the AMR and the magnet. However, continuous movement of an experimental device in a cryogenic environment often undermines its reliability. For a static AMRR, an alternating current (AC) low temperature superconducting (LTS) magnet was selected by previous researchers [10, 11] to create magnetic field variation. During the AMR experiment, a cryostat was filled with expensive liquid helium to remove heat from the LTS magnet caused by AC loss. Using liquid helium is neither an attractive nor efficient way for creating 20 K which enables a potential refrigeration system to liquefy hydrogen. In order to fabricate a cryogen-free system, a conduction cooled high temperature superconducting magnet must be prepared for operation above 20 K. This paper describes an AMRR operating between 80 K and 20 K with the conduction cooled HTS magnet. The AMR system including the AMR, the HTS magnet and the helium oscillating flow system is presented and the experimental results are discussed.

EXPERIMENTAL SETUP

Conduction cooled HTS magnet system

The HTS magnet system employed in this paper is a modified version of the previously studied magnet [13]. Figure 1 shows the overall HTS magnet system. Ramping current generated by a DC power supply (KLN 40-76, Kepco) is applied to the magnet by passing through the conduction cooled hybrid current leads. The hybrid current lead consists of HTS and copper current leads. Since

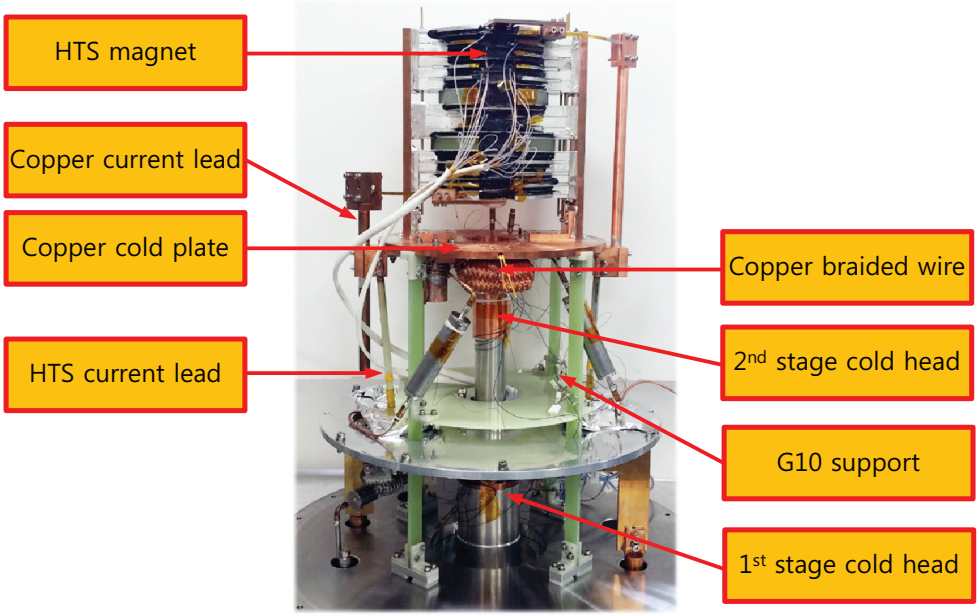

Figure 1. A photo of the HTS magnet system

AC flows through the magnet, heat generation due to AC loss has to be effectively minimized and dumped to the environment. The maximum heat generated by the magnet in the experiment is 12 W with the operating frequency of 0.1 Hz and the magnet is conductively cooled to 20 K by a two-stage GM cryocooler (RDK-415D, Sumitomo). Thermally conductive components such as copper braided wires, a copper plate and copper supports enable the cryocooler to cool the magnet with negligible temperature difference. The magnet is composed of twelve double pancake coils which are connected to each other by superconducting joints. Each double pancake coil was wound by GdBCO conductor insulated with polyimide tape. The HTS coils are thermally connected to aluminum plates and aluminum wings by Stycast 2850FT in order to effectively remove heat generated from the coils. The maximum central magnetic field of 3 T is produced when the current of 150 A is provided for the magnet whose diameter is 26 mm.

Active magnetic regenerator

The two stage AMR is composed of four different kinds of rare-earth compounds and shown in Fig. 2. The compounds are filled in the thin walled stainless steel tube with the inner diameter of 21.6 mm. The top end of the stainless steel tube is welded with a stainless steel flange. The stainless steel flange is mechanically fixed to an aluminum radiation shield by screws. Each compound is allocated by its primary transition temperature. $GdNi_2$ and $Dy_{0.85}Er_{0.25}Al_2$ which have relatively high transition temperatures are stacked in AMR1 while $Dy_{0.5}Er_{0.5}Al_2$ and $Gd_{0.1}Dy_{0.}9Ni_2$ are filled in AMR2 to cover low temperature region. A heater made by NiCr wire is installed in order to maintain the warm end of the AMR1 at 80 K. The filling ratio of the AMR is determined by a one-dimensional time dependent numerical model and the numerical results are indicated in Fig. 3. Each operation temperature of AMR1 or AMR2 is set to 80 - 45 K or 45 - 20 K by numerical simulation. Precise numerical calculation method is explained thoroughly in previous study [14]. Because the heat capacity of AMR1 is much higher than AMR2, the optimum shuttle mass for AMR1 is larger than AMR2. A bypass line made of 1/16 inch stainless steel tube is installed between AMR1 and AMR2 to control the amount of the shuttle mass for each AMR. Four calibrated temperature sensors (Cernox, Lakeshore) are installed on the external surface of the AMR to measure the temperature variation. The experimental apparatus including the AMR and the HTS magnet in the cryostat is evacuated below 10^{-4} torr during the experiment.

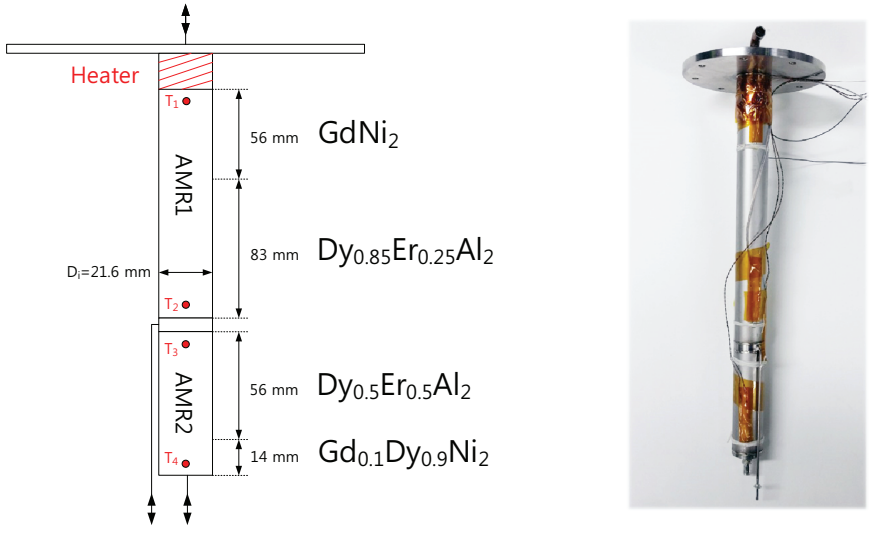

(a) (b)

Figure 2. (a) Schematic diagram and (b) a photo of the AMR

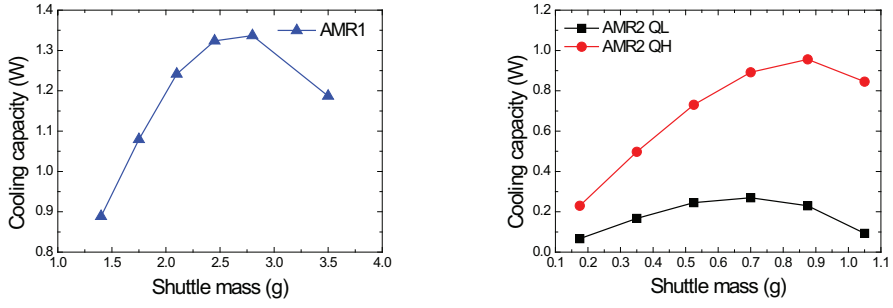

(a) (b)

Figure 3. Cooling capacity of (a) first (AMR1) and (b) second stage (AMR2) of the AMR calculated by numerical simulation.

Helium oscillation flow system

The helium gas oscillation flow system is illustrated in Fig. 4. The oscillating flow is provided by a helium compressor (M125, Austin Scientific) and two solenoid valves. Helium compressor generates a pressure difference and the inlet pressure (P1) changes by opening two solenoid valves alternatively. When periodic inlet pressure variation occurs, helium gas flows through the AMR and its shuttle mass is determined by the size of the buffer volumes, V1 and V2. Figure 5 shows the fabricated buffer tanks to create the desirable amount of oscillating flow. Since the helium gas with ambient temperature enters into the cryostat, the gas is cooled by the first stage of GM cryocooler. Moreover, passive regenerators (R1, R2, R3) are added at the oscillating helium flow line to reduce the cooling load of the cryocooler and AMR1.

EXPERIMENTAL CONDITIONS AND RESULTS

Experimental process and operating conditions

The experimental procedure is as follows:

1. Evacuate the AMR system for good thermal insulation.
2. Cool down the AMR system including the HTS magnet and the AMR by a cryocooler.
3. Proceed with HTS magnet test : continuous AC operation.
4. Oscillate helium gas flow.
5. Conduct the AMR experiment until the cyclic steady state is obtained.
6. Change the operating conditions.

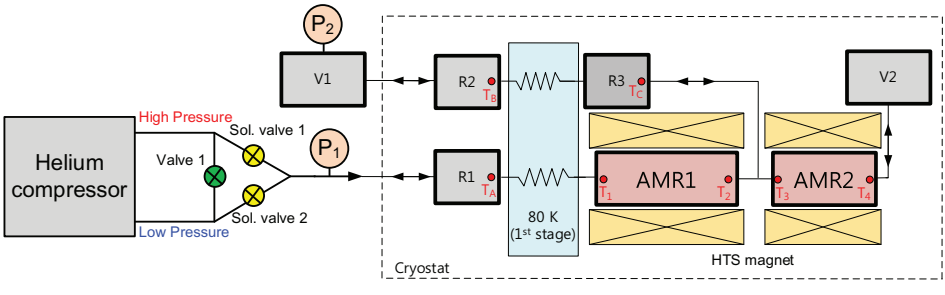

Figure 4. Helium gas oscillation flow system

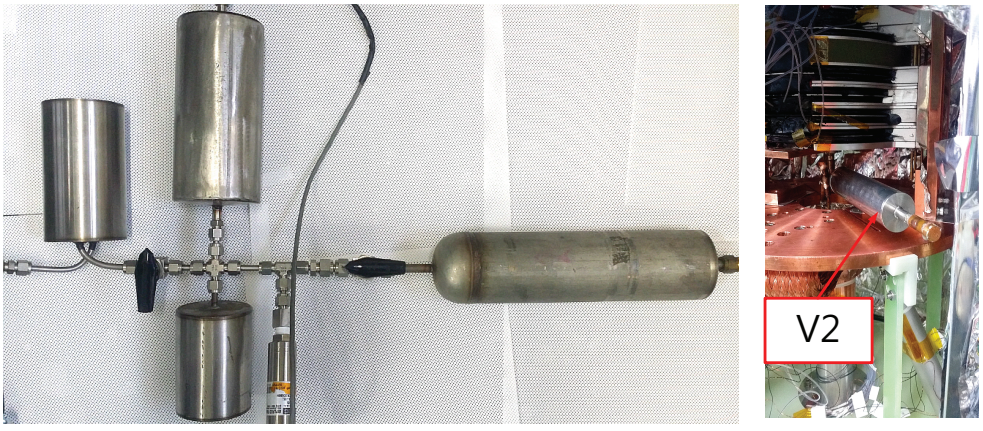

(a) (b)

Figure 5. Photo of the buffer volumes : (a) V1 composed of four stainless steel reservoirs and (b) V2 connected to the cold end of the AMR2

The helium gas flow and the magnet field variation during one cycle are illustrated in Fig. 6. The AMR is pseudo-adiabatically magnetized without helium flow at first. When the magnetic field reaches its maximum value, the up flow is induced so that the heat generated during the magnetization process is rejected through the top of the AMR. Next, the AMR is demagnetized in a pseudo-adiabatic manner to create low temperature. The down flow after demagnetization produces a cooling effect at the bottom of the AMR. Three experimental cases are reported in this paper. Ramping up or down time of the magnetic field is set to 3 seconds in all cases while the constant magnetic field times or the flow period of the three cases are specified as 7, 12, 17 seconds, respectively. The oscillating helium flow is generated during the constant magnetic field period to simulate magnetic reverse Brayton cycle. The maximum amplitude of buffer volumes' pressure swing (P2) which is in proportion to the amount of the shuttle mass is controlled by the helium flow time. The pressure swing amplitude increases as the gas flow time during half cycle lasts longer. The temperatures of the AMR, the pressures of the inlet and the buffer volume (V1) and the electric current supplied to the magnet are recorded at a rate of 10 samples per second using the Labview® program during the experiment. A summary of the operating conditions for three cases is presented in Table. 1.

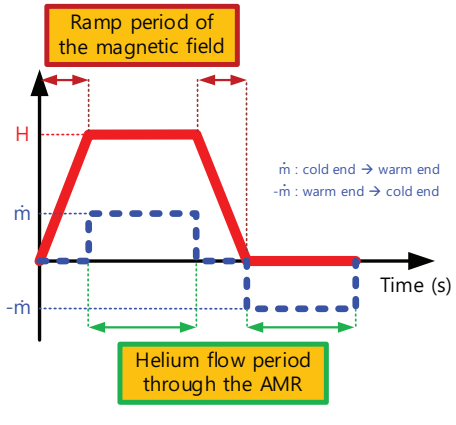

Figure 6. Magnetic field and mass flow rate variation during one cycle (the minus sign means down flow of the helium gas)

Table 1. Operating conditions of the AMR system

			Case 1	Case 2	Case 3
Cycle period (s)			20	30	40
Duration of mass flow during half cycle (s)			7	12	17
magnetization or demagnetization period (s)			3		
Buffer volume (m^3)		**V1**	2.79×10^{-3}		
		V2	4.83×10^{-5}		
Regenerator	**Length (m)**	**R1, R2**	0.2		
		R3	0.15		
	Diameter (m)	**R1, R2, R3**	0.248		
	Porosity (-)	**R1, R2, R3**	0.65		
P_1 (MPa)		**Max.**	1.3		
		Min.	0.3		
P_2 (MPa)		**Max.**	1.09	1.13	1.17
		Min.	0.76	0.67	0.58
Shuttle mass calculated by P_2 during half cycle (g)		**AMR1**	1.81	2.53	3.25
		AMR2	0.30	0.42	0.54

Experimental results and discussions

Figure 7 shows the temperature history of the AMR for Case 1. The warm end of the AMR1 (AMR1H) is cooled to 60 K by the first stage of the GM cryocooler at the beginning of the operation. During of the AMR operation, we can observe that the AMR temperature slowly decreases as shown in Fig. 7(a). A heater installed at the warm end of the AMR is turned on after the thermal cyclic steady state of the AMR is reached. The temperature of the AMR1H is held near 80 K by the heater as shown in Fig. 7(b). The no-load temperature spans and the lowest temperature of the AMR are 50.2 K and 28.3 K, respectively in Case 1. If the AMR does not experience magnetic field variation, the overall temperature of the AMR slowly rises and it can be observed in Fig. 7(b) after 18,000 seconds. The temperature variation during two cycles at the cyclic steady state is shown in Fig. 8(a). When the AMR is magnetized, the AMR temperature increases due to MCE. The cold ends of the AMR1(AMR1L) and AMR2(AMR2L) are cooled down by the upflow of the helium gas after magnetization. In contrast, the temperature of AMR1H slightly increases in upflow period. This

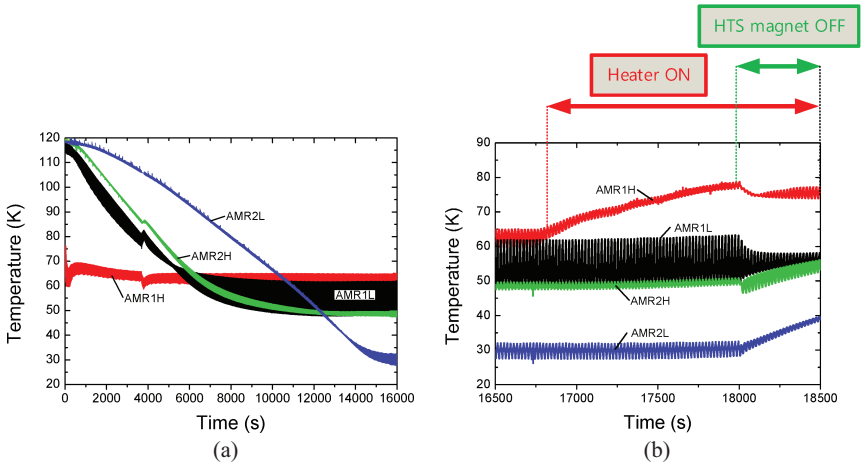

Figure 7. Temperature history of the AMR of case 1 (a) without heating (b) with heating of the AMR1H.

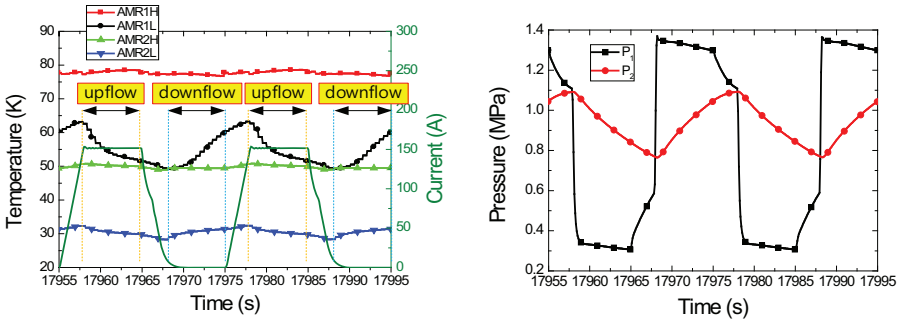

(a) (b)

Figure 8. (a) Temperature variation of the AMR and (b) pressure variation of the P1 and P2 during two cycles at case 1.

means that the AMR dumps heat at the warm end by the up flow of helium gas which exchanges heat with the magnetic refrigerant. The AMR is demagnetized after the up flow of the helium gas and its temperature decreases. Finally, the temperature of the AMR increases in the down flow period because the heated helium gas from the warm end flows through the AMR and exchanges heat with the magnetic refrigerants. The pressure swing of the inlet of the AMR (P_1) and V1 (P_2) is shown in Fig. 8(b). The pressure variation of P_1 is identical in all cases. However, the amplitude of P_2 depends on the flow duration. It is interesting to note that the temperature span of the AMR increases in accordance with the amount of shuttle mass, even though the operating frequency of the AMR system decreases. The largest temperature span of 59 K is achieved in case 3 and the result is shown in Fig. 9(b). The shuttle mass of AMR1 in case 2 was estimated as the amount for optimal performance of the AMR1 in the numerical results as shown in Fig. 3. However, the largest temperature span of the AMR1 is achieved in the case 3. This discrepancy can stem from the inefficiency of R3. Since R3 is not an ideal regenerator, the cold end of R3 connected with those of AMR1 deprives cooling capacity of AMR1 to maintain low temperature. The parasitic heat load by R3 is influenced by the operating frequency, the shuttle mass, and temperature span of R3. If V1 is installed in the cryostat by removing R2 and R3, we can directly compare the experimental results with the numerical results. The pressure swing of helium gas in V2 is not directly measured in this paper. If we assume the pressure swing in V2 is identical to that in V1, the shuttle mass of AMR2 can be estimated and the results are included in Table 1. Because the calculated shuttle masses in three cases are smaller than the optimal value (0.7 g) which is predicted by the numerical results of Fig. 3, the temperature span of AMR2 is expected to be further increased by transferring more shuttle mass of helium gas.

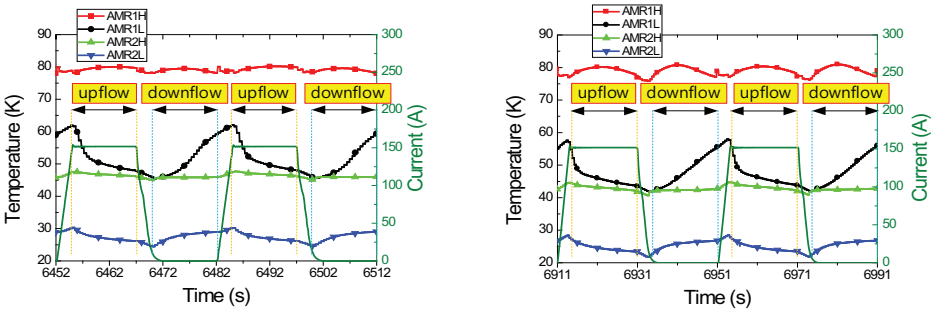

(a) (b)

Figure 9. Temperature variation of the AMR at (a) case 2 and (b) case 3

CONCLUSIONS

The multi-layered AMR operating between liquid nitrogen and hydrogen temperatures is designed, fabricated and tested. Four different kinds of magnetic refrigerants are arranged in the AMR bed. The cold end of the AMR reaches no-load temperature of 21.8 K and the maximum temperature span of 59 K is achieved. The performance of the AMR is investigated with various shuttle masses of helium gas. The temperature span of the AMR is increased with the increased the shuttle mass of helium. The numerical results predict that the performance of the AMR should decrease if the amount of the shuttle mass exceeds a certain value. In order to observe the performance tendency of the AMR, the buffer volumes (V1, V2) should be enlarged to increase the shuttle mass. Furthermore, the ineffectiveness of the auxiliary passive regenerator (R3) deteriorates the performance of the AMR1. Installation of the buffer volume, V1 in the cryostat will minimize heat leak at the cold end of the AMR1.

ACKNOWLEDGMENT

This research was supported by the Converging Research Center Program through the Ministry of Science, ICT and Future Planning, Korea (2014M3C1A8048836).

REFERENCES

1. Giauque, W.F.. MacDougall, D.P., “Attainment of temperatures below 1 K absolute by demagnetization of $Gd_2(SO_4)_3 \cdot 8H_2O$,” *Physics Review*, Vol. 43 (1933), pp. 768.
2. Gschneidner, K.A., Pecharsky, V.K., “Thirty years of near room temperature magnetic cooling: Where we are today and future prospects,," *International Journal of Refrigeration*, Vol.31 (2008), pp. 945-961.
3. Scarpa, F., Tagliafico, G., Tagliafico, L. A., “A classification methodology applied to existing room temperature magnetic refrigerators up to the year 2014," *Renewable and Sustainable Energy Reviews*, vol .50 (2015), pp. 497-503.
4. Yu, B., Liu, M., Egolf, P. W., Kitanovski A., “A review of magnetic refrigerator and heat pump prototypes built before the year 2010” *International Journal of Refrigeration*, Vol.33 (2010), pp. 1029-1060.
5. Jeong, S., Smith Jr, J. L., Iwasa Y., “Tandem magnetic refrigerator for 1.8 K," *Cryogenics*, Vol. 34 (1994), pp.263-269.
6. Cogswell, F.J., Iwasa, Y., Smith Jr, J. L., “A regenerative magnetic refrigerator operating between liquid helium and liquid hydrogen reservoirs," *IEEE Transactions on magnetics*, Vol. 24 (1988), pp. 1011-1014.
7. Seyfert, P., Bredy, P., Claudet, G., “Construction and testing of a magnetic refrigeration device for the temperature range of 5–15 K," *Proceedings of International Cryogenic Engineering Conference* (1988), pp. 607–611.
8. Numazawa, T., Kamiya, K., Utaki, T., Matsumoto, K., “Magnetic refrigerator for hydrogen liquefaction," *Cryogenics* , Vol. 62 (2014), pp.185-192.
9. Hirayama, Y., Okada, H., Nakagawa, T., Yamamoto, T., Kusunose, T., Numazawa, T., Mastumoto, K., Irie, T., Nakamura, E., “Experimental study of active magnetic regenerator (AMR) composed of spherical GdN," *Cryocoolers*, Vol.16 (2011), pp.531.
10. Kim, Y., Park, I., Jeong, S., “Experimental investigation of two-stage active magnetic regenerative refrigerator operating between 77 K and 20 K," *Cryogenics*, Vol. 57 (2013), pp. 113-121.
11. Park, I., Jeong, S., “Experimental investigation of 20 K two-stage layered active magnetic regenerative refrigerator," *IOP Conference Series: Materials Science and Engineering*, Vol. 101 (2015), pp.012106.
12. Jeong, S., “AMR (Active Magnetic Regenerative) refrigeration for low temperature," *Cryogenics*, Vol. 62 (2014), pp. 193-201
13. Park, I., Lee, C., Park, J., Kim, S., Jeong, S., “Ramping operation of the conduction-cooled high-temperature superconducting magnet for an active magnetic regenerator system," *IEEE Transactions on applied superconductivity*, Vol. 26 (2016), pp.4600505.

14. Park, I., Kim, Y., Park, J., Jeong, S., “Design method of the layered active magnetic regenerator (AMR) for hydrogen liquefaction by numerical simulation," *Cryogenics*, Vol. 70 (2015), pp.57-64.